

Strong pressure dependence of the magnetic penetration depth in single crystals of the heavy fermion superconductor CeCoIn₅ studied by muon spin rotation

L. Howald,^{1,*} A. Maisuradze,^{1,2} P. Dalmas de Réotier,³ A. Yaouanc,^{2,3}
C. Baines,² G. Lapertot,³ K. Mony,³ J.-P. Brison,³ and H. Keller¹

¹*Physik-Institut der Universität Zürich, Winterthurerstrasse 190, CH-8057 Zürich, Switzerland*

²*Laboratory for Muon Spin Spectroscopy, Paul Scherrer Institut, CH-5232 Villigen PSI, Switzerland*

³*Institut Nanosciences et Cryogénie, SPSMS, CEA and University Joseph Fourier, F-38054 Grenoble, France*

(Dated: August 18, 2018)

In the tetragonal heavy fermion system CeCoIn₅ the unconventional superconducting state is probed by means of muon spin rotation. The pressure dependence (0 – 1 GPa) of the basal-plane magnetic penetration depth (λ_a), the penetration depth anisotropy ($\gamma = \lambda_c/\lambda_a$) and the temperature dependence of $1/\lambda_i^2$ ($i = a, c$) were studied in single crystals. A strong decrease of λ_a with pressure was observed, while γ and $\lambda_i^2(0)/\lambda_i^2(T)$ are pressure independent. A linear relationship between $1/\lambda_a^2(270 \text{ mK})$ and T_c was also found. The large decrease of λ_a with pressure is the signature of an increase of the number of superconducting quasiparticles by a factor of about 2.

Unconventional superconductors are characterized by their proximity to different instabilities. In heavy fermion systems superconductivity is often found in the region of the phase diagram where a weak magnetic phase disappears [1]. However, in some systems [2] superconductivity is also detected in proximity of a valence phase transition.

CeCoIn₅ is a prototypical heavy fermion superconductor [3] at the focus of numerous studies owing to the proximity of quantum criticality. This proximity is reflected by the pronounced non-Fermi liquid features [4] and the highest superconducting (SC) transition temperature $T_c = 2.3 \text{ K}$ [3] among the Ce based heavy fermions. In addition, this tetragonal system is characterized by a quasi two-dimensional Fermi surface [5, 6] and a two-gap [7] unconventional SC state with d-wave symmetry [8].

In order to clarify the relation between the SC phase and quantum criticality, the evolution of basic SC parameters with respect to a tuning parameter is required. In this letter the pressure (p) and temperature (T) dependence of a fundamental SC quantity — the magnetic penetration depth (λ_i) — was studied. Here $i = a, c$ corresponds to a screening current flowing along the main crystallographic directions: perpendicular, respectively parallel to the c -axis. λ_i is obtained through the precise magnetic field distribution in the SC vortex state probed by transverse-field (TF) muon-spin rotation (μSR).

CeCoIn₅ is in the clean limit with a ratio of coherence length to mean free path $\xi/l < 0.02$ ($\xi < 8.2 \text{ nm}$) [5, 7]. In this limit the penetration depth can be written in the London model as:

$$1/\lambda_i^2 = \mu_0 e^2 n_S / m_i^* \quad (1)$$

Here μ_0 is the vacuum permeability, e the electron charge, n_S the number density (number of supercon-

ducting quasiparticles), and m_i^* the effective quasiparticle mass.

The μSR experiments were performed at the Swiss Muon Source (S μS), Paul Scherrer Institute (PSI), Switzerland, using the GPD (under p) and LTF (ambient p , low T) spectrometers. In a TF- μSR experiment spin polarized positive muons are implanted into a sample in an external magnetic field $\mu_0 H$ (field cooled from above T_c) applied perpendicular to the initial muon-spin polarization. In the presence of a magnetic field at the muon site B_μ the muon spin precesses at its Larmor frequency $\omega_\mu = \gamma_\mu B_\mu$ ($\gamma_\mu = 8.516 \cdot 10^8 \text{ rad s}^{-1} \text{T}^{-1}$ is the gyromagnetic ratio of the muon) before decaying with a life time of $\tau_\mu = 2.2 \mu\text{s}$ into a positron and two neutrinos. Due to parity violation the decay positron is preferentially emitted along the muon spin direction. Forward and backward positron detectors with respect to the initial muon polarization are used to monitor the μSR asymmetry spectrum $A(t)$.

Single crystals of CeCoIn₅ were grown by indium flux method [9] (rare earth from [10]), centrifuged and etched in HCl solution to remove the indium excess. Thin plate-like single crystals were obtained with their large faces corresponding to the (001) basal plane. Using this particular geometry, two samples were prepared, consisting of ~ 10 , respectively ~ 200 crystals glued together with G.E. varnish, as sketched in Fig. 2. The mosaic sample (c -axis normal to the plane) was studied with the LTF spectrometer. The cylindrical-like sample (a -axis is the main axis) was mounted in a piston cylinder pressure cell of CuBe alloy with Daphne oil as a pressure transmission medium [11] and measured with the GPD spectrometer. The actual pressure in the cell was determined by the T_c of a small piece of indium.

For different pressures an angular scan consisting of 5-8 TF- μSR spectra was taken at $T \simeq 270 \text{ mK}$ with an

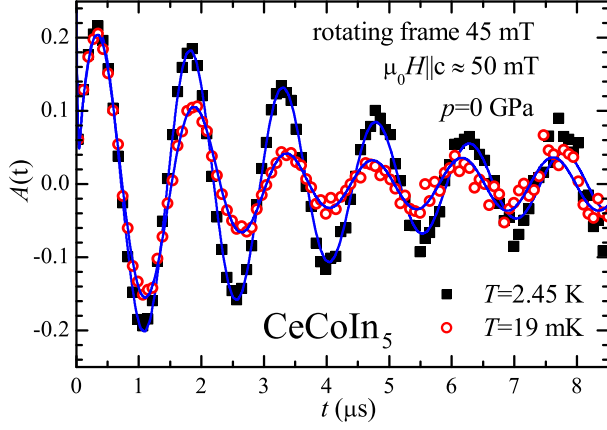


FIG. 1. (Color online) μ SR asymmetry spectrum $A(t)$ of CeCoIn_5 at ambient pressure in the normal (black squares) and SC state (red circles) taken with the LTF spectrometer at $\mu_0 H = 50$ mT for $H \parallel c$. The data are shown in a frame rotating at a frequency corresponding to 45 mT [14]. Solid lines represent fits to the data (see text).

applied field $\mu_0 H \simeq 50$ mT forming an angle θ with the sample's crystallographic c -axis. For $p = 0$ GPa, 0.2 GPa, and 0.6 GPa a temperature scan was also recorded for $\theta = 0^\circ$ ($H \parallel c$) and $\theta = 90^\circ$ ($H \perp c$). The field was chosen to be higher than the critical field of bulk indium ($\mu_0 H_{c2}(0) = 23$ mT) to avoid artifacts due to possible residual flux from the growth. For comparison the values of the Pauli limited critical fields for CeCoIn_5 are: $\mu_0 H_{c1} \simeq 10$ mT ($H \parallel c$ and $H \perp c$) [7], $\mu_0 H_{c2} = 5$ T ($H \parallel c$) and 11.5 T ($H \perp c$) [5]. A field of $\mu_0 H = 50$ mT is also small enough so that the Knight shift [12] and Zeeman current [13] effects can be neglected in the analysis of the spectra. In the normal state about $6 \cdot 10^6$ and in the SC state $10 - 20 \cdot 10^6$ positrons events were recorded for a μ SR time spectrum.

Typical TF- μ SR time spectra in the normal and SC state are displayed in Fig. 1. The temporal oscillations and damping of the μ SR asymmetry reflect directly the local magnetic field distribution at the muon stopping sites. The μ SR time spectrum consists of two contributions: a background signal (Bg) arising from the muons stopping in the silver sample holder for the LTF spectrometer or the pressure cell for the GPD spectrometer and a signal arising from the muons stopping in the sample (S) [11]. These contributions are clearly seen in Fig. 1. At short times the sample contribution dominates: in the SC state the damping of the signal is enhanced due to the field broadening generated by the vortex lattice (VL), and the oscillating frequency is reduced due to diamagnetic screening. In contrary, for $t > 7$ μ s in the normal state and $t > 3.5$ μ s in the SC state, only the signal of the muons stopping in the silver background persists. The μ SR time spectra are well described with

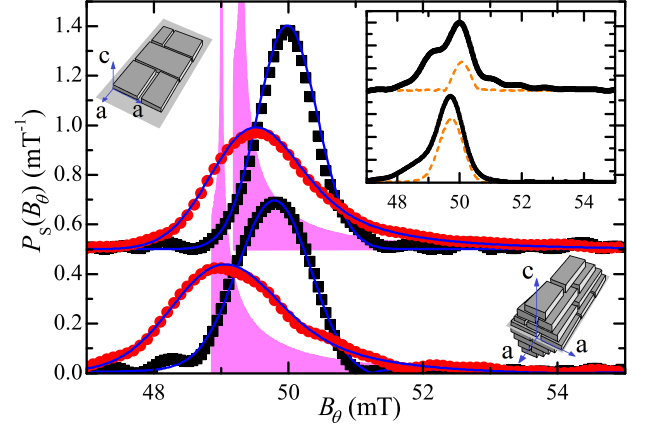


FIG. 2. (Color online) Local magnetic field distributions $P_S(B_\theta, T)$ of CeCoIn_5 at $\mu_0 H \approx 50$ mT for $H \parallel c$ in the normal (black squares) and SC (red circles) state obtained with the GPD (bottom; $p = 0.2$ GPa, $T \simeq 270$ mK) and the LTF (top; $p = 0$ GPa, $T \simeq 19$ mK) spectrometers. The blue lines are FT of $R_S(t)$. The magenta area represent $0.5P_{VL}(B_\theta, T)$. For clarity, the LTF field distributions are shifted vertically. A Gaussian apodization ($A(t) \exp[-1/2(t/\tau)^2]$) of $\tau = 4$ μ s (5 μ s) was used for the GPD (LTF) spectra. In the inset the FT of $A(t)$ (black lines) is shown. The orange dotted lines are the FT of $R_{Bg}(t)$.

the following equation:

$$A(t) = A_0[(1 - f_S(\theta))R_{Bg}(t) + f_S(\theta)R_S(t)] \quad (2)$$

Here $f_S(\theta)$ denotes the fraction of muons stopping in the sample, A_0 the initial asymmetry of the signal and $R_S(t)$ [$R_{Bg}(t)$] is the sample [background] muon depolarization function. $f_S(\theta)$ was determined to be $\simeq 82\%$ for the LTF spectrometer and typically $\simeq 45\%$ for the GPD spectrometer. Here $f_S(\theta)$ varies each time the pressure cell is manipulated (change of p or θ) as the sample position relative to the muon beam is modified. In various configurations we recorded a μ SR spectrum after a small field increase of 4 mT at low temperatures. Due to pinning the shift of field in the sample is less, allowing to determine precisely the fraction of muons stopping in the sample. The background depolarization function is described by a Gaussian field distribution [11]:

$$R_{Bg}(t) = \cos(\gamma_\mu \langle B_{Bg}(\theta, T) \rangle t + \phi_0) \exp(-\gamma_\mu^2 \sigma_{Bg}^2(\theta, T) t^2 / 2) \quad (3)$$

The average background magnetic field $\langle B_{Bg}(\theta, T) \rangle \simeq 50$ mT and the standard deviation of the Gaussian field distribution $\sigma_{Bg}(\theta, T)$ vary in the SC state since the diamagnetic sample induces a field inhomogeneity in its surrounding. The initial phase ϕ_0 is constant.

The sample depolarization function may be written as:

$$R_S(t) = \exp(-\gamma_\mu^2 \sigma_S^2(\theta, T) t^2 / 2) \times \int P_{VL}(B_\theta, T) \cos(\gamma_\mu B_\theta t + \phi_0) dB_\theta \quad (4)$$

The presence of a VL gives rise to a local magnetic field distribution along the direction of the applied field

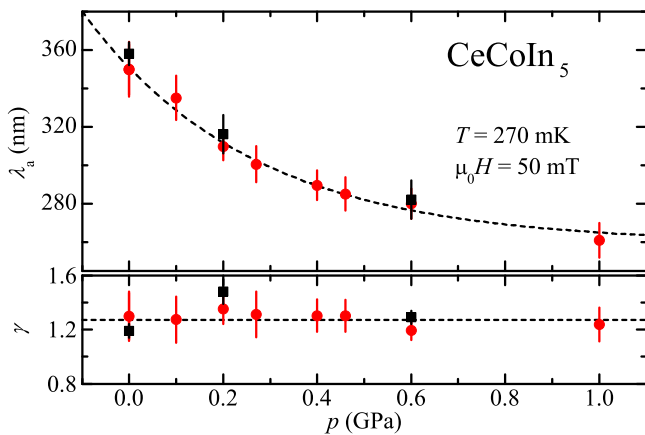


FIG. 3. (Color online) Pressure dependence of λ_a and $\gamma = \lambda_c/\lambda_a$ in CeCoIn₅. Red circles are obtained from angular dependent spectra, black squares from the temperature dependent ones. Dashed lines are guides for the eyes.

$P_{VL}(B_\theta, T)$, reflected by the integral in Eq. (4). For an extreme type-II superconductor in the London limit $P_{VL}(B_\theta, T)$ is uniquely determined by an effective penetration depth $\lambda_{eff}(\theta, T)$ [14, 15]. For the two principal magnetic field orientations one has: $\lambda_{eff}(\theta = 0^\circ, T) = \lambda_a(T)$ and $\lambda_{eff}(\theta = 90^\circ, T) = \sqrt{\lambda_a(T)\lambda_c(T)}$. The first factor in Eq. (4) describes the muon depolarization due to additional contributions ($\sigma_S^2(\theta, T) = \sigma_N^2(\theta) + \sigma_{dVL}^2(\theta, T)$) [16]: (i) the nuclear moments [$\sigma_N(\theta) \approx 0.5$ mT] and (ii) the disorder of the VL [$\sigma_{dVL}(\theta, T) = \sigma_{dVL0}(\theta)\lambda_{eff}^2(\theta, 0)/\lambda_{eff}^2(\theta, T)$ with $\sigma_{dVL0}(\theta) \approx 0.5$ mT [17]]. The local magnetic field distribution in the sample $P_S(B_\theta, T)$ can be obtained from the cosine Fourier transformation (FT) of the experimentally measured $A(t)$, after subtraction of $R_{Bg}(t)$ (Fig. 2).

The angular dependent spectra were analyzed globally [Eqs. (2) to (4)] [18] with the constraint that $\lambda_{eff}(\theta, T) = \lambda_a(T)\sqrt{\cos^2(\theta) + \gamma(T)\sin^2(\theta)}$ with $\gamma(T) = \lambda_c(T)/\lambda_a(T)$ [19]. $\lambda_{eff}(\theta, T = 270$ mK) was used to determine the exact orientation of the sample in the pressure cell (position of $\theta = 0^\circ$). The pressure dependence of the obtained parameters λ_a and γ are shown in Fig. 3 (red circles). The analysis of the temperature dependent spectra treated globally [18] is also presented (black squares). The two data sets give similar results, although different assumptions were made (T or θ dependence of some parameters fixed), demonstrating the reliability of the model.

The analysis yields at ambient pressure a value of $\lambda_a(T \rightarrow 0\text{K}, \mu_0 H = 50\text{mT}) = 350(12)$ nm. Since in the London model the contribution of the vortex core is neglected, this value is overestimated [20]. Taking $\mu_0 H_{c2Orb} \simeq 7.5$ T for the orbital upper critical field [21], this correction is only $\simeq 4\%$ for an applied field of $\mu_0 H = 50$ mT and therefore was neglected. In comparison, the first μ SR experiment reported $\lambda_a(0) \approx 550$ nm

[22]. This experiment was performed in a large magnetic field $\mu_0 H = 0.3$ T, and in the analysis an additional field broadening was neglected [16]. This is very likely the main reason for the larger value of $\lambda_a(0)$. Neutron diffraction experiments reported $\lambda_a(0)$ between 247(10) nm [23] and $\simeq 465$ nm [24]. The first value, measured in a magnetic field of 2 T, was underestimated because Zeeman currents that produce an additional contribution to the field broadening [25] were neglected. The second value was deduced from measurements at 0.5 T. Including the correction for the vortex cores [20], we obtain $\lambda_a(0) \approx 360$ nm in agreement with the present value. Surface impedance techniques provided smaller $\lambda_a(0) \approx 260$ nm [26] and $\lambda_a(0) = 281(14)$ nm [27]. These experiments were performed in an extremely low magnetic field ($< 10\mu\text{T}$) in the Meissner state.

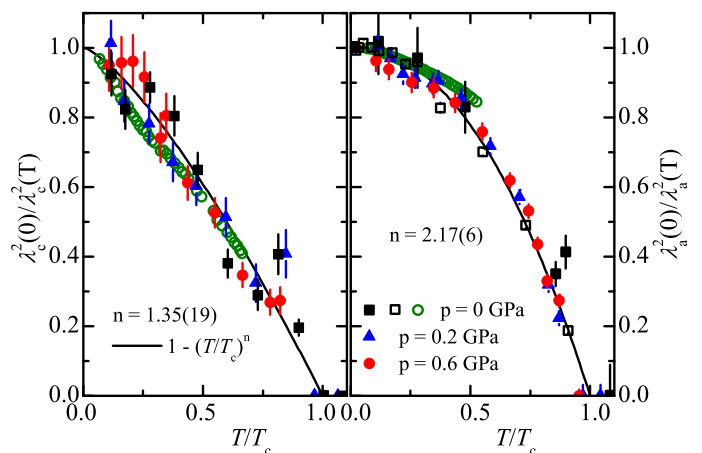


FIG. 4. (Color online) $\lambda_i^2(0)/\lambda_i^2(T)$ for the two main orientations $i = a, c$ for CeCoIn₅. Interestingly, $\lambda_i^2(0)/\lambda_i^2(T)$ is pressure independent in the range investigated. Full symbol were taken with the GPD spectrometer, empty squares with the LTF spectrometer. The empty green circles are obtained from tunnel-diode oscillator experiments adapted from Ref. [26]. Black lines are power law fits to the data as described in the text.

The temperature dependence of $\lambda_i^2(0)/\lambda_i^2(T)$ ($i = a, c$) is displayed in Fig. 4, together with a fit of the form $1 - (T/T_c)^n$. The pressure evolution of T_c was determined independently by SQUID magnetometry (Fig. 5). The exponent n was found to be $n = 2.17(6)$ for $i = a$ in agreement with Ref. [28], while $n = 1.35(19)$ for $i = c$. Similar temperature dependences can be obtained using $\Delta\lambda_i = \lambda_i(T) - \lambda_i(0)$ measured by tunnel-diode oscillator experiments [26] taking $\lambda_a(0) \simeq 336$ nm and $\lambda_c(0) \simeq 421$ nm from this work (green empty circles in Fig. 4). Within precision both $\lambda_i^2(0)/\lambda_i^2(T)$ ($i = a, c$) are pressure independent, suggesting that the gap symmetry is unchanged, and the value of the gap to T_c ratio is constant, in agreement with the variation of less than 10% obtained by NQR [29] in this pressure range.

The pressure independent value of $\gamma = \sqrt{m_c^*/m_a^*} \simeq 1.3$

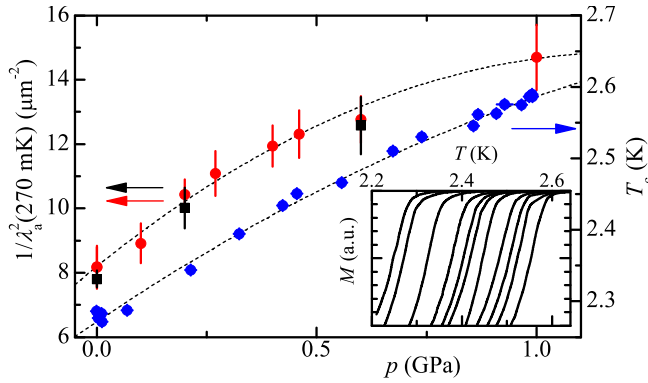


FIG. 5. (Color online) Pressure dependence of $1/\lambda_a^2(270 \text{ mK})$ (left scale, same symbol convention as in Fig. 3) measured by μSR and T_c (right scale) determined by SQUID magnetometry of CeCoIn_5 . Dashed lines are parabolic pressure dependences. Inset: magnetization curves recorded at selected pressures and used to determine T_c (T_c criterion is the onset of the transition).

(Fig. 3) is in good agreement with the constant value deduced from the initial slope of the upper critical field under pressure $H'_{c2}(H \perp c, p)/H'_{c2}(H \parallel c, p) \propto m_c^*/m_a^* \approx 2$ [21, 30]. The same experiments indicate that the variation of m^* with pressure is less than 10% between 0-1 GPa with a maximum around 0.5 GPa. Such a small variation cannot explain the pressure dependence of $1/\lambda_a^2$ plotted in Fig. 5. Therefore, we conclude that, within the London model [Eq. (1)], n_S increases with pressure. Using an average value $m_a^* \approx 50m_0$ [5] one obtains from Eq. (1) a change of n_S from $n_S \approx 1.8$ to 3.4 carriers per unit cell between 0 and 1 GPa.

In the following we discuss two possible scenarios for this strong increase of n_S . The first one relies on the proposed multigap SC state of CeCoIn_5 [7]. The observed increase of n_S with pressure would result from an increase of the small gap at 50 mT. Indeed, at ambient pressure for $\mu_0 H \approx 50 \text{ mT}$ the smaller gap is already closed [7]. To check whether the small gap could open under pressure, we probed the field dependence of the total magnetic field standard deviation in the sample σ_D . Here $\sigma_D^2 = \sigma_S^2 + (0.06092\Phi_0/\lambda^2)^2$ [14] is the quadratic sum of σ_S previously defined and the magnetic field standard deviation generated by the VL (Φ_0 is the flux quantum). For comparison, for the two-gap superconductor $\text{PrOs}_4\text{Sb}_{12}$ [31] different slopes $d\sigma_D/dH$ are observed between the low magnetic field regime with two opened SC gaps and the high magnetic field regime where only one SC gap is present [32]. In CeCoIn_5 , the fact that the magnetic field dependence of σ_D is the same at 0 GPa and 0.6 GPa (inset Fig. 6), strongly suggests that a single gap is probed in the full pressure range.

Another scenario is based on an increase of the Ce valence (orbital occupancy $n_V \approx 0.9$ [33] at ambient pressure). Such a scenario was proposed for the parent com-

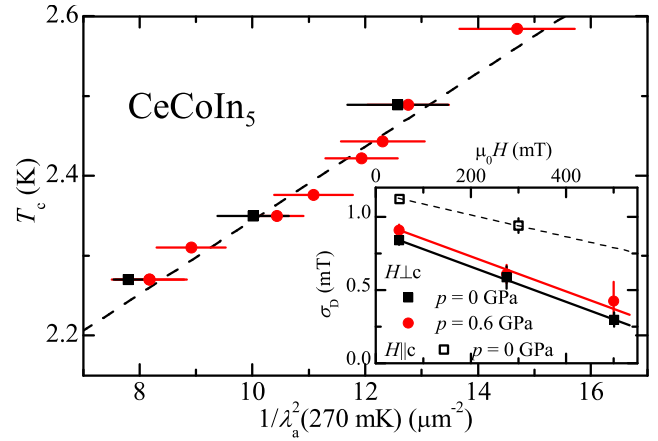


FIG. 6. (Color online) Plot of T_c versus $1/\lambda_a^2(270 \text{ mK})$ for CeCoIn_5 under pressure (same symbol convention as in Fig. 3). A linear relation (dashed line $T_c(\lambda_a) = T_{c0} + A/\lambda_a^2$) with $T_{c0} = 1.88(3) \text{ K}$ and $A = 4.6(3) \cdot 10^{-2} \text{ K}\mu\text{m}^2$ is found. Inset: field dependence of the magnetic field standard deviation σ_D (see text for details).

pound CeRhIn_5 where a similar decrease of λ_a is observed between $p = 2.07 \text{ GPa}$ and $p = 2.26 \text{ GPa}$ [34]. Note that valence fluctuations are often associated with SC in Ce based heavy fermions [35].

An interesting observation is the linear relation $T_c(\lambda_a) = T_{c0} + A/\lambda_a^2(270 \text{ mK})$ shown in Fig. 6. This relation has some analogy with the Uemura plot [$T_c(\lambda_a) = A_U/\lambda_a^2(0)$] [36] found for underdoped cuprate superconductors and other electronically doped unconventional superconductors. However, substantial differences exist: (i) no proportionality ($T_{c0} \neq 0$) and (ii) A is about 90 times smaller than A_U . In addition, pressure affects $1/\lambda_a^2$ much more in CeCoIn_5 than in cuprates [11].

In conclusion, we show by TF- μSR that in CeCoIn_5 the magnetic penetration depth (λ_a) decreases under pressure, while the anisotropy ($\gamma = \lambda_c/\lambda_a$) and the temperature dependence of the penetration depth ratios $\lambda_a^2(0)/\lambda_a^2(T)$ and $\lambda_c^2(0)/\lambda_c^2(T)$ are almost unaffected. In the range of pressure investigated, a linear dependence between T_c and $1/\lambda_a^2$ was found. Within the London model, the decrease of $\lambda_a(270 \text{ mK})$ under pressure corresponds to a doubling of the number density (n_S) between 0 and 1 GPa, possibly related with the presence of a quantum critical point.

This work was performed at the Swiss Muon Source ($S\mu\text{S}$), Paul Scherrer Institut (PSI), Switzerland. We acknowledge support by the Swiss National Science Foundation and the NCCR Program MaNEP.

* ludovic.howald@physik.uzh.ch

[1] N. Mathur *et al.*, Nature **394**, 39 (1998).

[2] D. Jaccard *et al.*, Physica B **259-261**, 1 (1999).

- [3] C. Petrovic *et al.*, J. Phys.: Condens. Matter **13**, L337 (2001).
- [4] V. A. Sidorov *et al.*, Phys. Rev. Lett. **89**, 157004 (2002); Y. Nakajima *et al.*, J. Phys. Soc. Jpn. **76**, 024703 (2007).
- [5] R. Settai *et al.*, J. Phys.: Condens. Matter **13**, L627 (2001).
- [6] T. Maehira *et al.*, J. Phys. Soc. Jpn. **72**, 854-864 (2003).
- [7] G. Seyfarth *et al.*, Phys. Rev. Lett. **101**, 046401 (2008).
- [8] K. Izawa *et al.*, Phys. Rev. Lett. **87**, 057002 (2001); H. Aoki *et al.*, J. Phys.: Condens. Matter **16**, L13 (2004).
- [9] P. Canfield and Z. Fisk, Philos. Mag. B **65**, 1117 (1992).
- [10] Rare earth purified at the Materials Preparation Center, Ames Laboratory, US DOE Basic Energy Sciences, Ames, IA, USA. See: www.mpc.ameslab.gov.
- [11] A. Maisuradze *et al.*, Phys. Rev. B **84**, 184523 (2011).
- [12] W. Higemoto *et al.*, J. Phys.: Conf. Ser. **225**, 012013 (2010).
- [13] J. Spehling *et al.*, Phys. Rev. Lett. **103**, 237003 (2009); P. Dalmas de Réotier and A. Yaouanc, Phys. Rev. B **84**, 012503 (2011).
- [14] A. Yaouanc and P. Dalmas de Réotier, *Muon Spin Rotation, Relaxation, and Resonance: Applications to Condensed Matter*, International Series of Monographs on Physics (Oxford University Press, 2011).
- [15] E. H. Brandt, J. Low Temp. Phys. **73**, 355 (1988); A. Maisuradze *et al.*, J. Phys.: Condens. Matter **21**, 075701 (2009).
- [16] The presence of two different muon stopping sites with different Knight shifts produces a broadening proportional to the applied field: $\sigma_K \approx 0.2$ mT at 50 mT in the normal phase. This broadening which is reduced by a factor nearly 2 [12] in the SC state is negligible at 50 mT compared to the other contributions, but it is not for sizably larger fields.
- [17] T. M. Riseman *et al.*, Phys. Rev. B **52**, 10569 (1995).
- [18] Explicitly, this means that all the spectra taken at a given p and T for different θ or at a given p and θ for different T are fitted together with the constraints given in the text. Each point of the asymmetry spectrum $A(t)$ is weighted statistically.
- [19] L. N. Bulaevskii, M. Ledvij, and V. G. Kogan, Phys. Rev. B **46**, 366 (1992).
- [20] A. Yaouanc, P. Dalmas de Réotier, and E. H. Brandt, Phys. Rev. B **55**, 11107 (1997).
- [21] L. Howald *et al.*, New J. Phys. **13**, 113039 (2011).
- [22] W. Higemoto *et al.*, J. Phys. Soc. Jpn. **71**, 1023-1026 (2002).
- [23] M. R. Eskildsen *et al.*, Phys. Rev. Lett. **90**, 187001 (2003).
- [24] A. D. Bianchi *et al.*, Science **319**, 177 (2008).
- [25] V. P. Michal and V. P. Mineev, Phys. Rev. B **82**, 104505 (2010).
- [26] E. E. M. Chia *et al.*, Phys. Rev. B **67**, 014527 (2003).
- [27] S. Özcan *et al.*, EPL (Europhysics Letters) **62**, 412 (2003).
- [28] V. G. Kogan, R. Prozorov, and C. Petrovic, J. Phys.: Condens. Matter **21**, 102204 (2009).
- [29] M. Yashima *et al.*, J. Phys. Soc. Jpn. **73**, 2073 (2004).
- [30] G. Knebel *et al.*, Phys. Status Solidi B **247**, 557 (2010).
- [31] G. Seyfarth *et al.*, Phys. Rev. Lett. **95**, 107004 (2005).
- [32] D. E. MacLaughlin *et al.*, Phys. Rev. Lett. **89**, 157001 (2002).
- [33] C. H. Booth *et al.*, Phys. Rev. B **83**, 235117 (2011).
- [34] R. H. Heffner *et al.*, J. Phys.: Conf. Ser. **225**, 012011 (2010).
- [35] S. Watanabe and K. Miyake, J. Phys.: Condens. Matter **23**, 094217 (2011).
- [36] Y. J. Uemura *et al.*, Phys. Rev. Lett. **66**, 2665 (1991).